ULTRA SONO GRAPHY

A superficial hyperechoic band in human articular cartilage on ultrasonography with histological correlation: preliminary observations

Tae Sun Han[1,2], Kyu-Sung Kwack[1,2], Sunghoon Park[1,2], Byoung-Hyun Min[3,4], Seung-Hyun Yoon[4], Hyun Young Lee[5,6], Kyi Beom Lee[7]

[1]Department of Radiology, Ajou University School of Medicine, Suwon; [2]Musculoskeletal Imaging Laboratory, Ajou University Medical Center, Suwon; [3]Department of Orthopedic Surgery, Ajou University School of Medicine, Suwon; [4]Cartilage Regeneration Center and [5]Regional Clinical Trial Center, Ajou University Medical Center, Suwon; [6]Department of Biostatistics, Yonsei University College of Medicine, Seoul; [7]Department of Pathology, Ajou University School of Medicine, Suwon, Korea

Purpose: To demonstrate the superficial hyperechoic band (SHEB) in articular cartilage by using ultrasonography (US) and to assess its correlation with histological images.

Methods: In total, 47 regions of interest (ROIs) were analyzed from six tibial osteochondral specimens (OCSs) that were obtained after total knee arthroplasty. Ultrasonograms were obtained for each OCS. Then, matching histological sections from all specimens were obtained for comparison with the ultrasonograms. Two types of histological staining were used: Safranin-O stain (SO) to identify glycosaminoglycans (GAG) and Masson's trichrome stain (MT) to identify collagen. In step 1, two observers evaluated whether there was an SHEB in each ROI. In step 2, the two observers evaluated which histological staining method correlated better with the SHEB by using the ImageJ software.

Results: In step 1 of the analysis, 20 out of 47 ROIs showed an SHEB (42.6%, kappa=0.579). Step 2 showed that the SHEB correlated significantly better with the topographical variation in stainability in SO staining, indicating the GAG distribution, than with MT staining, indicating the collagen distribution ($P<0.05$, kappa=0.722).

Conclusion: The SHEB that is frequently seen in human articular cartilage on high-resolution US correlated better with variations in SO staining than with variations in MT staining. Thus, we suggest that a SHEB is predominantly related to changes in GAG. Identifying an SHEB by US is a promising method for assessing the thickness of articular cartilage or for monitoring early osteoarthritis.

Keywords: Cartilage; Ultrasonography; Knee joint; Histology

ORIGINAL ARTICLE

http://dx.doi.org/10.14366/usg.14047
pISSN: 2288-5919 • eISSN: 2288-5943
Ultrasonography 2015;34:115-124

Received: October 19, 2014
Revised: December 27, 2014
Accepted: December 28, 2014

Correspondence to:
Kyu-Sung Kwack, MD, Department of Radiology, Ajou University School of Medicine, 164 World cup-ro, Yeongtong-gu, Suwon 443-380, Korea

Tel. +82-31-219-5852
Fax. +82-31-219-5862
E-mail: xenoguma@ajou.ac.kr

How to cite this article:
Han TS, Kwack KS, Park S, Min BH, Yoon SH, Lee HY, et al. A superficial hyperechoic band in human articular cartilage on ultrasonography with histological correlation: preliminary observations. Ultrasonography. 2015 Apr; 34(2):115-124.

Introduction

Ultrasonography (US) is a useful and convenient diagnostic tool for the musculoskeletal system. Indeed, US is commonly used to diagnose various knee joint conditions, including osteoarthritis (OA). US is also used for evaluating the articular cartilage of the knee joint, although there are some areas where US cannot be used to evaluate the articular cartilage within the knee joint [1–8]. Sonographic assessment of cartilage damage in patients with OA is also important for early diagnosis and for monitoring responses to therapy [9]. By the early 1980s, US was being used to evaluate knee joint cartilage [3]. At the time, a transducer with a frequency of <10 MHz was used [3]. To date, most studies have reported on the usefulness of US in measuring articular cartilage thickness; articular cartilage is seen as a homogeneous anechoic or hypoechoic band-like structure on US [2–8].

During research on articular cartilage in our laboratory, we have found that there is a superficial hyperechoic band (SHEB) that is seen frequently on US (Fig. 1), and that it may have a different meaning than the hyperechoic superficial interface or echogenic anterior margin seen in the past [3–6,8,10,11]. If so, it was worth investigating whether it would be insufficient to measure only the depth of the anechoic band for the thickness of articular cartilage or to evaluate only the anechoic layer for early OA. To the best of our knowledge, no previous report in the English literature about an SHEB on ultrasonograms has been published. Thus, we performed this study to demonstrate the US findings of an SHEB and to assess any correlation with histological images.

Materials and Methods

Subjects

This study was approved by the Institutional Review Board of our hospital. Osteochondral specimens from patients who underwent total knee arthroplasty (TKA) and that were stored at our institution were examined to obtain appropriate samples. The lateral tibial condyle was chosen for examination because it had less OA-related cartilage degeneration. Some specimens were excluded on the basis of the following criteria: morphology of the cartilage was defective due to fragmentation of the specimen, when more than half of the cartilage was eroded (International Cartilage Repair Society [ICRS] grades 3 and 4), the patient had underlying neoplastic or rheumatological disease(s), or the patient had a history of trauma, fracture, or surgery of the knee joint. In the end, six osteochondral specimens were selected for the study. Of these six specimens, five were from female patients, and one was from a male patient (mean age, 63.3 years; range, 46 to 81 years). Seven to nine regions of interest (ROIs) were selected per osteochondral specimen; thus, 47 ROIs were analyzed.

Specimen Preparation

The osteochondral specimens were placed in jars filled with normal saline and were delivered to our laboratory within a few hours after surgery. Each specimen was immediately refrigerated at 4°C before examination.

US Examination

Ultrasonograms were obtained with an Acuson Sequoia 512 ultrasound system (Siemens Medical Solutions, Mountain View, CA, USA) by using a 17-MHz multifrequency linear array transducer. All sonographic examinations were performed by a single experienced musculoskeletal radiologist. The radiologist was instructed to obtain orthogonal mid-sagittal images from the lateral tibial condyle of each osteochondral specimen. Great care was taken to maintain the US plane of the section as consistently as possible. The gain setting was individually optimized for each osteochondral specimen

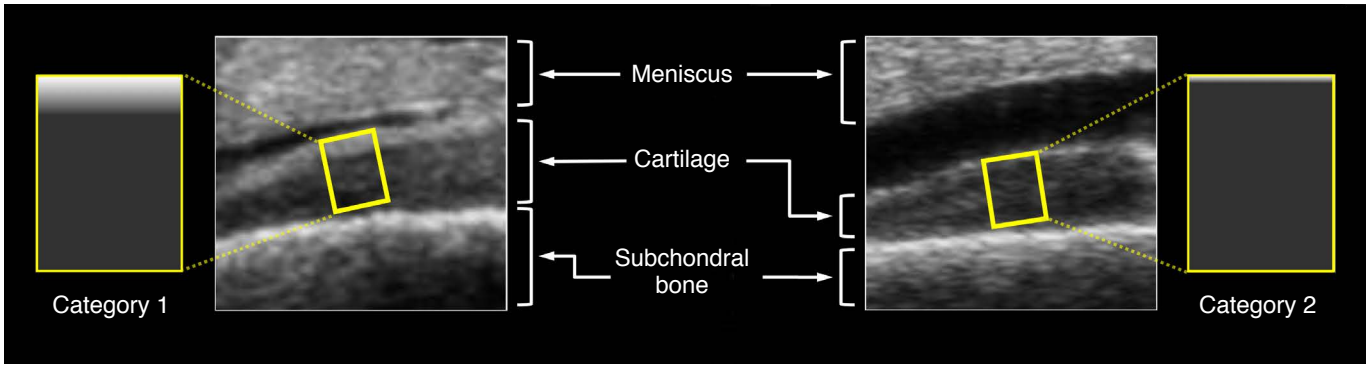

Fig. 1. **Sonograms acquired from osteochondral specimens and schematic representation to show dichotomized patterns of echogenicity at each region of interest (ROI) (yellow rectangular boxes) in the articular cartilage.** The left ROI shows a superficial hyperechoic band, defined as category 1. The right ROI shows a homogeneous hypoechoic pattern, defined as category 2.

by using equalized automatic gain control. Markings were made on each specimen to be used as references for the histological sections to exactly match the ultrasonograms. Multiple mid-sagittal images were taken at the same midline of the lateral tibial condyle to select the optimal ultrasonograms that would most closely match the histological slides from the next step. All ultrasonograms were transferred to an independent workstation (Mac Pro, Apple Inc., Cupertino, CA, USA).

Histology

The specimens were fixed in 10% buffered formalin and decalcified in 10% formic acid. After decalcification, the specimens were sectioned through the middle of the lateral tibial condyle in the true sagittal plane, corresponding to the sagittal plane used for US imaging. The location of the histological section was chosen using both the previously made markings and measurements from anatomical and pathological landmarks, such as the lateral margin of the tibial plateau, the tibial spine, and osteophytes

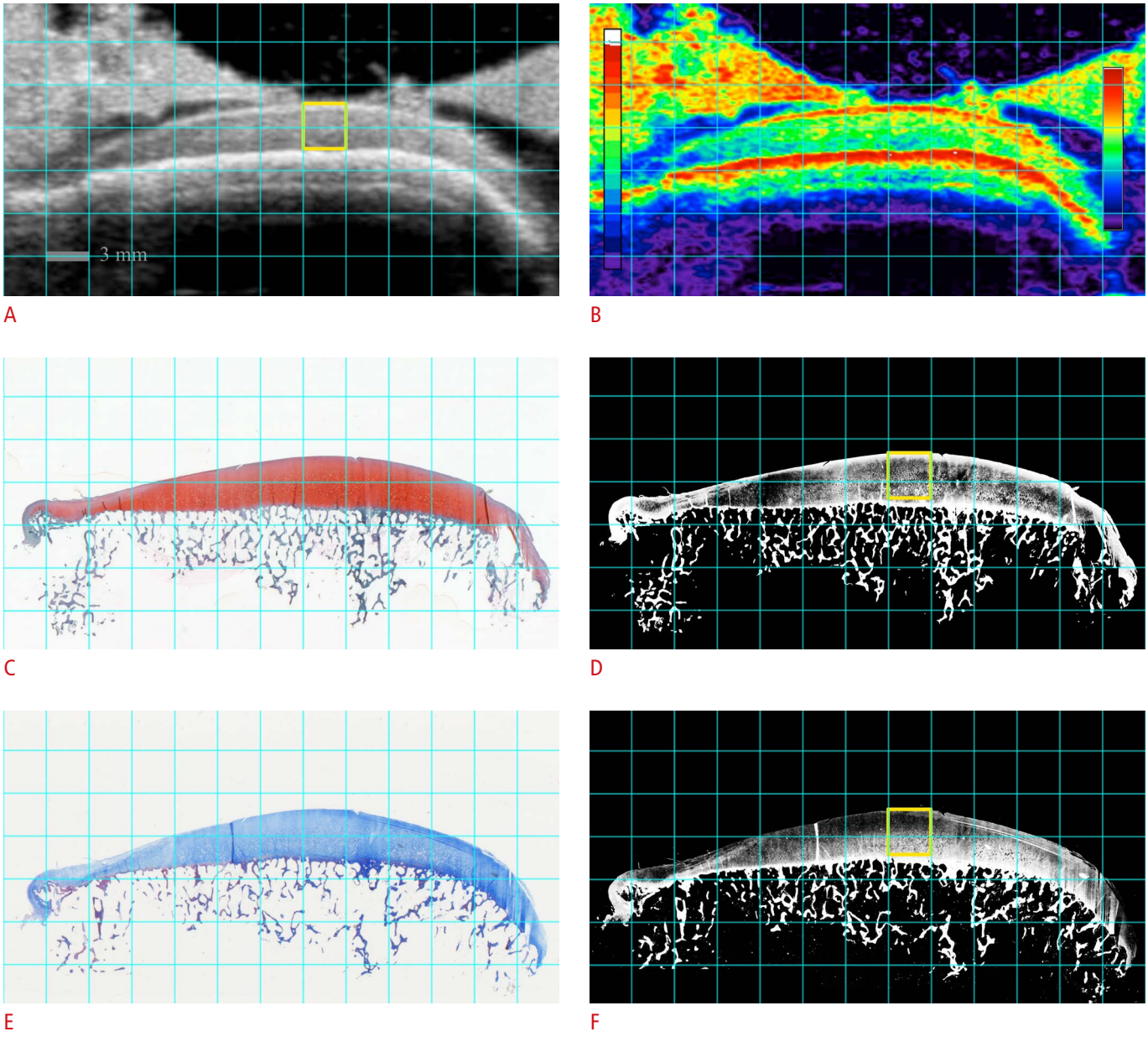

Fig. 2. An osteochondral specimen from 45-year-old male patient who underwent total knee arthroplasty.
A, B. A sonogram (A) and a color-coded sonogram (B) show a thin superficial hyperechoic band (SHEB) at the articular cartilage. C–F. The sonogram and histological images are matched: Safranin-O stain (SO) (C), SO_R (D), Masson's trichrome stain (MT) (E), and MT_B (F). The SO_R image (D) shows thin glycosaminoglycan depletion at the superficial layer of the articular cartilage.

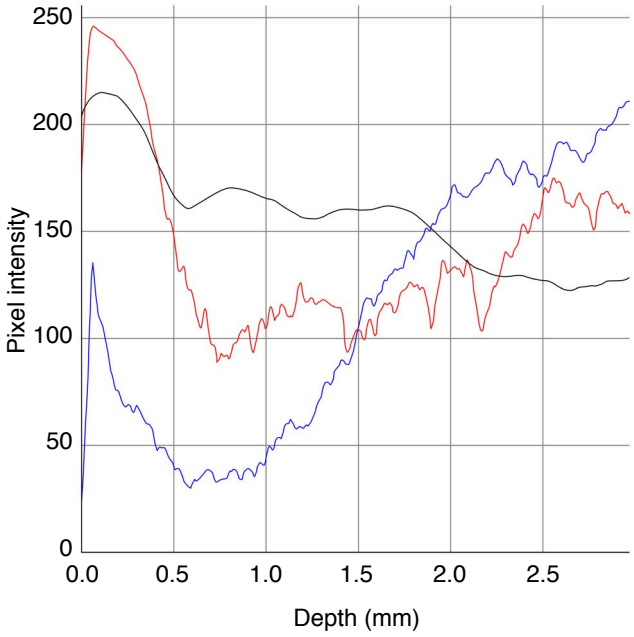

G

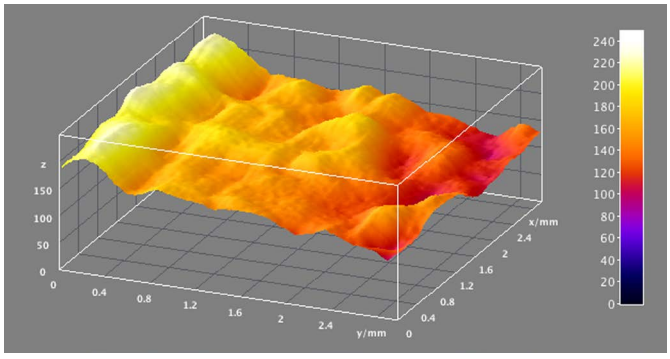

H

Fig. 2. G. A vertical profile plot shows the pixel intensities of each region of interest (ROI) along the depth of the articular cartilage: red curve (pixel intensity of ROI on SO_R), black curve (pixel intensity of ROI on sonogram), and blue curve (pixel intensity of ROI on MT_B). H. The SHEB is also visualized as an elevated bright band on a three-dimensional surface plot, reconstructed from the pixel intensities of the sonogram.

[12,13]. The tissue was subsequently embedded in paraffin wax, and 4-μm sections were made using a microtome (RM2255, Leica Microsystems, Wetzlar, Germany). Two sections of each lateral tibial condyle were stained with both Safranin-O (SO) and Masson's trichrome (MT) stain in pairs (Figs. 2C, 2E, 3C, 3E). SO staining was used to identify glycosaminoglycans (GAG), a major component of proteoglycans (PG), and MT staining was used to identify collagen [14–18].

Image Processing

A color CMOS camera mounted on a binocular microscope (Eclipse 55i, Nikon Instruments Inc. Melville, NY, USA) and Adobe Photoshop CS6 (Adobe Systems, San Jose, CA, USA) were used for digital RGB image processing and merging. All microscopic images of the histological slides were captured with the same LED light and exposure parameters (Fig. 1).

The red color in the SO-stained histological image showed topographical variation and the content of GAG on the histological slides. Thus, the red channel of the SO-stained histological image was extracted and converted into grayscale images, making it comparable with the echogenicity on ultrasonograms. During the histological image processing from each osteochondral specimen, the equalization function of Photoshop was used to equalize the brightness and contrast of all converted images. The converted grayscale images show black pixels for empty spaces on the histological slide, lower pixel intensity at the outer layer of the cartilage, and higher intensity at the inner layer of the cartilage, which was the opposite of the echogenicity of the ultrasonograms. Thus, a grayscale inversion step was needed to assist with the correlation between the echogenicity of the ultrasonograms and the pixel intensity of the histological images. This final image, obtained after image processing, was named the "SO_R" image (Figs. 2D, 3D). In the MT-stained histological images, the blue color showed the topographical variation and content of collagen. Thus, the blue channel of the MT-stained histological image was similarly converted to a grayscale image, which was named the "MT_B" image (Figs. 2F, 3F).

To exactly match the histological image and ultrasonogram, an optimal mid-sagittal ultrasonograms was carefully selected from multiple stored mid-sagittal images on the basis of morphological features, such as anatomical landmarks, osteophytes, thickness of cartilage, and edge-distance measurements [12,13]. During the whole image processing procedure, the size ratios of all images were kept the same and the resolution of each image was fixed at 4,096 pixels in width. A 3-mm interval grid was applied to each image set of each osteochondral specimen to position the ROIs at the same location in each image. Seven to nine ROIs were positioned with grids on sagittal sections for a more focused comparison between the echogenicity of the ultrasonograms and the pixel intensity of the grayscale histological images (SO_R and MT_B) [12,13]. This was performed in consensus by a bone pathologist and a musculoskeletal radiologist. When positioning ROIs, they were located away from areas where deep fissures, histology processing artifacts, and US artifacts, such as microbubble shadowing, were

present. The width of each ROI was 2–4 mm. Finally, 47 ROIs were selected from the six osteochondral specimens for the analysis. Color-coded ultrasonograms with a consistent color look-up table (Figs. 2B, 3B) were generated from ultrasonograms on an independent workstation by using DICOM imaging software (OsiriX, Pixmeo, Geneva, Switzerland).

For step 2 of the image analysis, ImageJ software (US National Institute of Health, Bethesda, MD, USA) was used. Three vertical profile plots were generated for the same ROIs for each ultrasonograms, the SO_R image, and the MT_B image (Figs. 2G, 3G). Twenty vertical profile plots were generated from the 20 ROIs that were selected in step 1. The vertical profile plot shows the topographical changes of pixel intensity along the depth from the cartilage surface (Figs. 2G, 3G). Three-dimensional (3D) surface plots

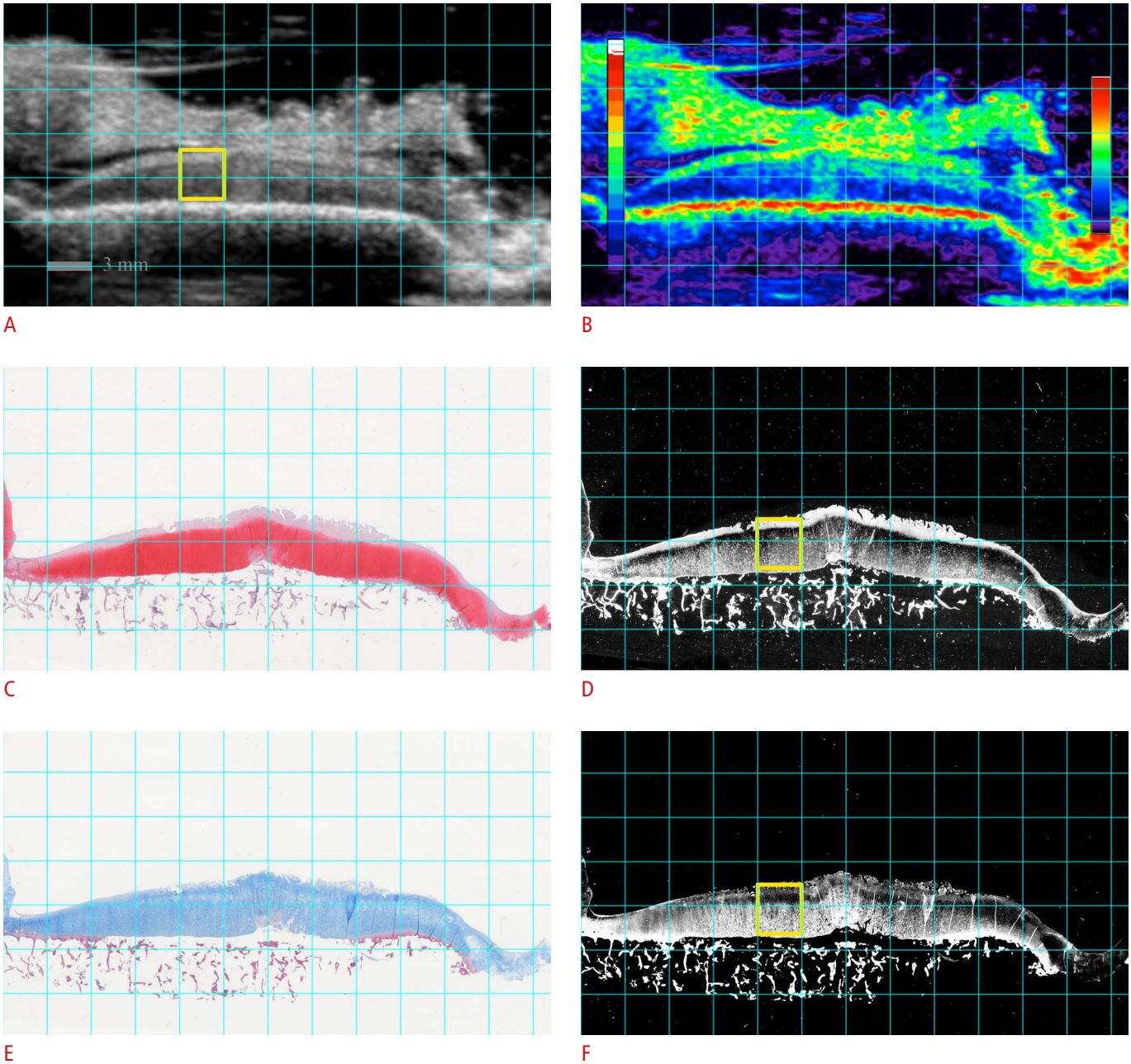

Fig. 3. An osteochondral specimen from a 56-year-old female patient who underwent total knee arthroplasty.
A, B. The sonogram (A) and color-coded sonogram (B) show a superficial hyperechoic band (SHEB) at the articular cartilage. C–F. The sonogram and histological images are matched: Safranin-O stain (SO) (C), SO_R (D), Masson's trichrome stain (MT) (E), and MT_B(F). The SO_R image (D) shows glycosaminoglycan depletion at the superficial layer of the articular cartilage.

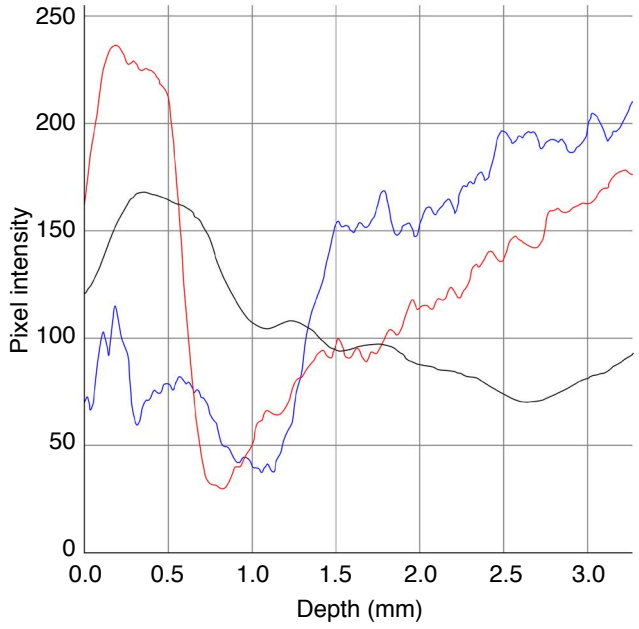

G

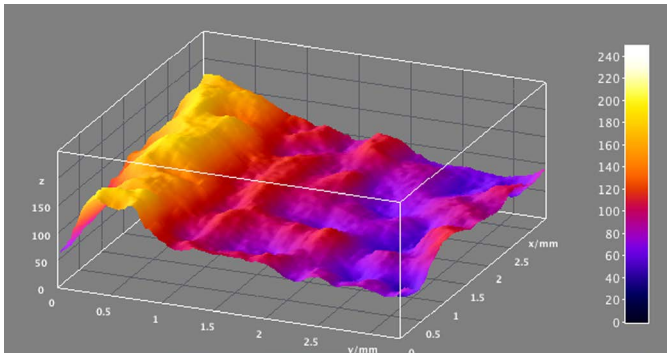

H

Fig. 3. G. A vertical profile plot shows the pixel intensities of each region of interest (ROI) along the depth of articular cartilage: red curve (pixel intensity of ROI on SO_R), black curve (pixel intensity of ROI on sonogram), and blue curve (pixel intensity of ROI on MT_B). H. The SHEB is visualized as an elevated bright band on the three-dimensional surface plot, which is reconstructed from the pixel intensities of the sonogram.

were generated to display 3D topographical pixel intensities from ROIs on the ultrasonograms (Figs. 2H, 3H).

Image Analysis

The image analysis was performed in two steps. Written instructions were provided to each observer prior to each step of the image analysis.

Step 1

The purpose of step 1 was to assess the incidence of SHEBs in all ROIs of the articular cartilage from our osteochondral specimens. The ROIs that showed an SHEB would be used in step 2. Thus, we classified the patterns of echogenicity at the ROIs into the following three categories (Fig. 1):

1. SHEB pattern
2. Hypoechoic pattern (homogeneously hypoechoic articular cartilage with no SHEB)
3. Indeterminate

If there was an SHEB at the superficial layer of the articular cartilage, the ROI was defined as category 1 (SHEB pattern) (Fig. 1). The meniscus was used as the reference standard for echogenicity because the meniscus is well known as a homogeneously hyperechoic structure [19]. Thus, an SHEB was defined as a superficial echogenic band that was isoechoic to or more hyperechoic than the meniscus. Thus, the SHEB was also hyperechoic to the deep layer of the articular cartilage. Category 2 (hypoechoic pattern) was defined as the ROI showing homogeneous hypoechogenicity relative to the meniscus and no incidence of SHEBs (Fig. 1). The hypoechoic pattern included the conventional hypoanechoic pattern that has been known to be representative of the echogenicity in the articular cartilage [2–8]. Category 3 (indeterminate) was defined as an ROI showing complex echogenicity that could not be classified into category 1 or 2.

A research assistant prepared multiple image sets composed of two types of ultrasonograms from each osteochondral specimen. One was a usual grayscale ultrasonogram (Figs. 2A, 3A), and the other was a color-coded ultrasonogram (Figs. 2B, 3B) for an improved comparison of echogenicity. Each image set contained grids that were used to localize the ROIs. Two observers (musculoskeletal radiologists A and B) were asked separately which pattern was seen for each of the 47 ROIs in the ultrasonograms. Each observer's preference was recorded as category 1, 2, or 3 by the assistant on a data sheet [20,21].

Step 2

The ROIs that both observers classified into category 1 in consensus in step 1 were selected for step 2. Another image set of ROIs, selected from step 1, were made for step 2 of the analysis. Each image set contained rectangular ROI images from the ultrasonograms, SO_R images, and MT_B images, and vertical profile plots that were generated from each ROI by using ImageJ for improved objectivity (Figs. 2G, 3G). There were three types of curves on the vertical profile plot. The curves showed the changes in pixel intensities along the depth in the ultrasonograms, SO_R images, and

MT_B images (Figs. 2G, 3G) to assist in objective decision-making.

After a 2-week "washout" period after step 1, a research assistant presented each image set to the two observers in a random order on a computer monitor. The observers were blinded to the type of histological staining, because grayscale ROI images that had been prepared from the channel-separated histological images (SO_R and MT_B) were displayed, and not the original histological images in color.

The two observers were asked separately which grayscale histological image (SO_R or MT_B) best correlated with the SHEB on the US for each of the 20 ROIs. The two standards of judgment on the vertical profile plot were (1) the proximity between the peak point of the US pixel intensity curve and the histological images' pixel intensity curve, and (2) the similarity of curve shape within the superficial layer of cartilage (Figs. 2G, 3G). Each observer's decision was classified into one of the following three categories and recorded by the assistant [20,21]:

1. SO_R profile (SHEB correlates to SO_R)
2. MT_B profile (SHEB correlates to MT_B)
3. Indeterminate

Statistical Analysis

Statistical analyses were performed using SPSS ver. 20.0 (IBM Co., Armonk, NY, USA) and the R statistical package ver. 2.10.1 R (Foundation for Statistical Computing, Vienna, Austria). The incidence for SHEB was calculated in step 1. In step 2, the proportion test was used to assess the statistical significance of differences in numbers among categories according to the observers' decisions [22,23]. Kappa values were calculated to assess the interobserver agreement for steps 1 and 2. A P-value of <0.05 was considered to indicate statistical significance. As suggested by Landis and Koch, agreement was considered poor when k<0, slight when k=0–0.2, fair when k=0.21–0.40, moderate when k=0.41–0.60, substantial when k=0.61–0.80, and almost perfect when k=0.81–1 [24].

Results

Step 1: Incidence of SHEBs in ROIs of Articular Cartilages in OA Patients

In total, 47 ROIs were selected from the ultrasonograms of osteochondral specimens. The 47 ROIs were investigated independently by the two observers. The incidence of SHEBs in all ROIs and the interobserver agreement are summarized in Table 1. The interobserver agreement was moderate (k=0.579) (Table 1). The number of ROIs that were answered as category 1 in consensus by both observers was 20 out of 47 (42.6%). All six osteochondral specimens had at least one ROI that showed SHEBs on ultrasonograms.

Step 2: The Grayscale Histological Image That Correlated Better with the SHEB on the Ultrasonograms

From step 1, 20 ROIs were selected for step 2. The 20 ROIs were investigated by two observers. Each observer's decision and the interobserver agreement are summarized in Table 2. The interobserver agreement was substantial (k=0.722) (Table 2). The number of ROIs that were classified into category 1 (SO_R) in consensus by both observers was 15 out of 20 (75.0%). No ROI was judged as category 2 (MT_B) by agreement. The difference in proportion was statistically significant (P<0.05). Thus, this result indicates that the SHEB correlated better with changes in staining in SO_R images than with those in MT_B images.

Table 1. Cross tabulation of step 1 results to show the incidence of SHEBs in the ROIs of articular cartilage and the interobserver agreement

Observer category		Observer A			Total	Kappa
		Category 1	Category 2	Category 3		
Observer B	Category 1	20 (42.6)	5	5	30	0.579
	Category 2	0	12 (25.5)	2	14	
	Category 3	0	0	3 (6.4)	3	
Total		20	17	10	47	

Values are presented as number (%).
Category 1, superficial hyperechoic band (SHEB); Category 2, hypoechoic pattern (homogeneously hypoechoic articular cartilage without SHEB); Category 3, indeterminate.
ROI, region of interest.

Table 2. Cross tabulation of step 2 results to show the interobserver agreement and the SHEB that correlated with histological staining (SO_R and MT_B)

Observer category		Observer A			Total	Kappa
		Category 1	Category 2	Category 3		
Observer B	Category 1	15 (75)	0	1	16	0.722
	Category 2	0	0 (0)	0	0	
	Category 3	0	1	3 (15)	4	
Total		15	1	4	20	

Values are presented as number (%).
Category 1, Safranin-O stain (SO) profile (superficial hyperechoic band [SHEB] correlates with SO_R); Category 2, Masson's trichrome stain (MT) profile (SHEB correlates with MT_B); Category 3, indeterminate.

Discussion

Most previous studies have reported the usefulness of US to measure articular cartilage thickness, and articular cartilage is typically seen as a homogeneous anechoic or hypoechoic band-like structure on US [2–8]. While examining osteochondral specimens using high-resolution US, we suspected that the thin superficial layer was sometimes more hyperechoic than the deep layer of the articular cartilage. We became interested in the topographical zonal variations that caused the superficial and deep layers of the articular cartilage to appear with differing echogenicity and in the constituent(s) of the articular cartilage that affected the echogenicity. The purposes of this study were to demonstrate findings of the SHEB in the articular cartilage, and to assess any correlation between the topographical changes in echogenicity and the constituents of articular cartilage.

The step 1 results showed that the incidence of SHEBs was 42.6% among the ROIs (Table 1). Past reports have described US figures of the articular cartilage as an anechoic band-like layer with a hyperechoic outer contour. Similar sonographic images can be seen in the reports, but most studies have reported that the hyperechoic outer superficial layer of the articular cartilage is either the synovial-cartilage interface, soft tissue-cartilage interface, hyperechoic superficial interface, echogenic anterior margin, or water-cartilage interface [1,3–6,8,10,11]. In our study, ultrasonograms of the articular cartilage showed a thin band-like superficial hyperechoic layer (SHEB). The SHEB was not the synovial-cartilage interface or an artifact because the osteochondral specimens in our study were placed in normal saline-filled jars with no synovial tissue and were evaluated using a high-resolution transducer. Razek et al. [9] noted that the blurring and poor visualization of the outer margin of the cartilage, loss of cartilage transparency, and increased echogenicity may reflect structural alterations. Grassi et al. [6] asserted that the loss of clarity in cartilage bands is an early sonographic feature of OA.

It is important to understand that articular cartilage is not a simple homogenous anechoic structure but a complex structure that can show topographical changes in echogenicity with SHEBs. This information may prevent investigators from potentially underestimating the thickness of the articular cartilage during a US examination, because many investigators define cartilage thickness as the width of only the anechoic space [1,2,7].

Articular cartilage is a complex structure with interactions among its biochemical constituents that include water, electrolytes, and a solid matrix composed primarily of collagens and GAG. The earliest signs of OA include the loss of PG and the disruption of the superficial collagen network, leading to the fibrillation of the articular cartilage surface [25]. The major macromolecule is GAG, a major component of PG. Some magnetic resonance imaging studies have asserted that variations in the water or PG content determine the layering within the articular cartilage, and topographical variations in the GAG content and the cartilage thickness have been reported [26–31]. Paul et al. [32] showed that the variation curve in the magnetic resonance signal intensity resembles the curve for zonal variation in the cartilage PG content, but not the curve for collagen or free-water content. Although there has been controversy about the relationship between US echogenicity and the constituents of articular cartilage in previous reports [33–38], in our study, we used high-resolution clinical US, B-mode images, and human osteochondral specimens and methods differentiated from these past studies. For objective analyses, specialized image processing was also used, based on the red color density on SO staining reflecting the distribution of GAG and the blue color density on MT staining reflecting the distribution of collagen [14–18].

In step 2 of the analysis of the set of 20 ROI images, category 1 was chosen more than the other categories by the two observers (Table 2). Thus, this finding indicates that the SHEB correlated better with the changes in staining on SO_R images than those on MT_B images (Figs. 2, 3). Our results suggest that the SHEB on US may reflect the depletion of GAG at the superficial layer of the articular cartilage (Figs. 2C, 2G, 2H, 3C, 3G, 3H). This result is consistent with that of Laasanen et al. [36] in that the US reflection parameters were not significantly related to the superficial collagen content. There are also other reports that ultrasound can be used for characterizing articular structural properties, such as surface roughness and PG depletion [37,39,40].

Our study has several limitations. This was a preliminary study with a small number of osteochondral specimens. Although all cartilage specimens in our study had at least one ROI that showed an SHEB, we cannot be sure whether healthy or young cartilage would show similar topographical changes because all osteochondral specimens in our study were obtained from OA patients who had undergone TKA. If the SHEB is not seen or is very thin in healthy and young individuals, the existence or thickening of the SHEB may be a promising subject for investigators studying the pathogenesis of OA and may provide an early sign of OA prior to the thinning of the articular cartilage itself. Another limitation is that the criteria for the minimum thickness of the SHEB for category 1 were not defined in our study. Therefore, the dichotomizations in step 1 were performed on the basis of visual perceptions by observers.

In conclusion, our study using human osteochondral specimens showed that articular cartilage is not a simple anechoic structure and that an SHEB is frequently seen at the articular cartilage. Our results also showed that an SHEB in articular cartilage correlated

with the changes in the red color channel of SO staining. Thus, our preliminary study suggests that an SHEB indicates the depletion of GAG at the superficial layer of the articular cartilage. Further studies are needed to investigate its correlation and usefulness in assessing cartilage degeneration.

ORCID: Tae Sun Han: http://orcid.org/0000-0003-1404-1578; Kyu-Sung Kwack: http://orcid.org/0000-0001-6124-8948; Sunghoon Park: http://orcid.org/0000-0003-0844-0521; Byoung-Hyun Min: http://orcid.org/0000-0001-8928-414X; Seung-Hyun Yoon: http://orcid.org/0000-0003-1787-7282; Hyun Young Lee: http://orcid.org/0000-0003-4169-8284; Kyi Beom Lee: http://orcid.org/0000-0002-1743-7829

Conflict of Interest

No potential conflict of interest relevant to this article was reported.

Acknowledgments

This study was supported by a grant from the Korea Healthcare Technology R&D Project, Ministry for Health, Welfare, and Family Affairs, Republic of Korea (A091120).

References

1. Naredo E, Acebes C, Moller I, Canillas F, de Agustin JJ, de Miguel E, et al. Ultrasound validity in the measurement of knee cartilage thickness. Ann Rheum Dis 2009;68:1322-1327.
2. Yoon CH, Kim HS, Ju JH, Jee WH, Park SH, Kim HY. Validity of the sonographic longitudinal sagittal image for assessment of the cartilage thickness in the knee osteoarthritis. Clin Rheumatol 2008;27:1507-1516.
3. Aisen AM, McCune WJ, MacGuire A, Carson PL, Silver TM, Jafri SZ, et al. Sonographic evaluation of the cartilage of the knee. Radiology 1984;153:781-784.
4. Disler DG, Raymond E, May DA, Wayne JS, McCauley TR. Articular cartilage defects: in vitro evaluation of accuracy and interobserver reliability for detection and grading with US. Radiology 2000;215:846-851.
5. Grassi W, Filippucci E, Farina A. Ultrasonography in osteoarthritis. Semin Arthritis Rheum 2005;34(6 Suppl 2):19-23.
6. Grassi W, Lamanna G, Farina A, Cervini C. Sonographic imaging of normal and osteoarthritic cartilage. Semin Arthritis Rheum 1999;28:398-403.
7. Castriota-Scanderbeg A, De Micheli V, Scarale MG, Bonetti MG, Cammisa M. Precision of sonographic measurement of articular cartilage: inter- and intraobserver analysis. Skeletal Radiol 1996;25:545-549.
8. Friedman L, Finlay K, Jurriaans E. Ultrasound of the knee. Skeletal Radiol 2001;30:361-377.
9. Razek AA, Fouda NS, Elmetwaley N, Elbogdady E. Sonography of the knee joint. J Ultrasound 2009;12:53-60.
10. Kim HK, Babyn PS, Harasiewicz KA, Gahunia HK, Pritzker KP, Foster FS. Imaging of immature articular cartilage using ultrasound backscatter microscopy at 50 MHz. J Orthop Res 1995;13:963-970.
11. Tsai CY, Lee CL, Chai CY, Chen CH, Su JY, Huang HT, et al. The validity of in vitro ultrasonographic grading of osteoarthritic femoral condylar cartilage: a comparison with histologic grading. Osteoarthritis Cartilage 2007;15:245-250.
12. Saadat E, Jobke B, Chu B, Lu Y, Cheng J, Li X, et al. Diagnostic performance of in vivo 3-T MRI for articular cartilage abnormalities in human osteoarthritic knees using histology as standard of reference. Eur Radiol 2008;18:2292-2302.
13. Kim T, Min BH, Yoon SH, Kim H, Park S, Lee HY, et al. An in vitro comparative study of T2 and T2* mappings of human articular cartilage at 3-Tesla MRI using histology as the standard of reference. Skeletal Radiol 2014;43:947-954.
14. Melrose J, Smith S, Ghosh P. Histological and immunohistological studies on cartilage. Methods Mol Med 2004;101:39-63.
15. Yoshioka H, Haishi T, Uematsu T, Matsuda Y, Anno I, Echigo J, et al. MR microscopy of articular cartilage at 1.5 T: orientation and site dependence of laminar structures. Skeletal Radiol 2002;31:505-510.
16. Yoo HJ, Hong SH, Choi JY, Lee IJ, Kim SJ, Choi JA, et al. Contrast-enhanced CT of articular cartilage: experimental study for quantification of glycosaminoglycan content in articular cartilage. Radiology 2011;261:805-812.
17. Schmitz N, Laverty S, Kraus VB, Aigner T. Basic methods in histopathology of joint tissues. Osteoarthritis Cartilage 2010;18 Suppl 3:S113-S116.
18. Takeuchi N, Suzuki Y, Sagehashi Y, Yamaguchi T, Itoh H, Iwata H. Histologic examination of meniscal repair in rabbits. Clin Orthop Relat Res 1997;(338):253-261.
19. Bianchi S, Martinoli C. Ultrasound of the musculoskeletal system. Berlin: Springer, 2007.
20. Floyd CE Jr, Baker JA, Chotas HG, Delong DM, Ravin CE. Selenium-based digital radiography of the chest: radiologists' preference compared with film-screen radiographs. AJR Am J Roentgenol 1995;165:1353-1358.
21. Balassy C, Prokop M, Weber M, Sailer J, Herold CJ, Schaefer-Prokop C. Flat-panel display (LCD) versus high-resolution gray-scale display (CRT) for chest radiography: an observer preference study. AJR Am J Roentgenol 2005;184:752-756.
22. Riddell AM, Khalili K. Assessment of acute abdominal pain: utility of a second cross-sectional imaging examination. Radiology 2006;238:570-577.
23. Cascade PN, Gross BH, Kazerooni EA, Quint LE, Francis IR, Strawderman M, et al. Variability in the detection of enlarged mediastinal lymph nodes in staging lung cancer: a comparison of contrast-enhanced and unenhanced CT. AJR Am J Roentgenol 1998;170:927-931.

24. Kundel HL, Polansky M. Measurement of observer agreement. Radiology 2003;228:303-308.
25. Viren T, Saarakkala S, Kaleva E, Nieminen HJ, Jurvelin JS, Toyras J. Minimally invasive ultrasound method for intra-articular diagnostics of cartilage degeneration. Ultrasound Med Biol 2009;35:1546-1554.
26. Bacic G, Liu KJ, Goda F, Hoopes PJ, Rosen GM, Swartz HM. MRI contrast enhanced study of cartilage proteoglycan degradation in the rabbit knee. Magn Reson Med 1997;37:764-768.
27. Paul PK, O'Byrne E, Blancuzzi V, Wilson D, Gunson D, Douglas FL, et al. Magnetic resonance imaging reflects cartilage proteoglycan degradation in the rabbit knee. Skeletal Radiol 1991;20:31-36.
28. Lehner KB, Rechl HP, Gmeinwieser JK, Heuck AF, Lukas HP, Kohl HP. Structure, function, and degeneration of bovine hyaline cartilage: assessment with MR imaging in vitro. Radiology 1989;170:495-499.
29. Kiviranta I, Tammi M, Jurvelin J, Helminen HJ. Topographical variation of glycosaminoglycan content and cartilage thickness in canine knee (stifle) joint cartilage: application of the microspectrophotometric method. J Anat 1987;150:265-276.
30. Olivier P, Loeuille D, Watrin A, Walter F, Etienne S, Netter P, et al. Structural evaluation of articular cartilage: potential contribution of magnetic resonance techniques used in clinical practice. Arthritis Rheum 2001;44:2285-2295.
31. Lammentausta E, Kiviranta P, Nissi MJ, Laasanen MS, Kiviranta I, Nieminen MT, et al. T2 relaxation time and delayed gadolinium-enhanced MRI of cartilage (dGEMRIC) of human patellar cartilage at 1.5 T and 9.4 T: Relationships with tissue mechanical properties. J Orthop Res 2006;24:366-374.
32. Paul PK, Jasani MK, Sebok D, Rakhit A, Dunton AW, Douglas FL. Variation in MR signal intensity across normal human knee cartilage. J Magn Reson Imaging 1993;3:569-574.
33. Senzig DA, Forster FK, Olerud JE. Ultrasonic attenuation in articular cartilage. J Acoust Soc Am 1992;92(2 Pt 1):676-681.
34. Laasanen MS, Toyras J, Vasara AI, Hyttinen MM, Saarakkala S, Hirvonen J, et al. Mechano-acoustic diagnosis of cartilage degeneration and repair. J Bone Joint Surg Am 2003;85 Suppl 2:78-84.
35. Pellaumail B, Watrin A, Loeuille D, Netter P, Berger G, Laugier P, et al. Effect of articular cartilage proteoglycan depletion on high frequency ultrasound backscatter. Osteoarthritis Cartilage 2002;10:535-541.
36. Laasanen MS, Saarakkala S, Toyras J, Rieppo J, Jurvelin JS. Site-specific ultrasound reflection properties and superficial collagen content of bovine knee articular cartilage. Phys Med Biol 2005;50:3221-3233.
37. Laasanen MS, Toyras J, Hirvonen J, Saarakkala S, Korhonen RK, Nieminen MT, et al. Novel mechano-acoustic technique and instrument for diagnosis of cartilage degeneration. Physiol Meas 2002;23:491-503.
38. Cherin E, Saied A, Laugier P, Netter P, Berger G. Evaluation of acoustical parameter sensitivity to age-related and osteoarthritic changes in articular cartilage using 50-MHz ultrasound. Ultrasound Med Biol 1998;24:341-354.
39. Toyras J, Rieppo J, Nieminen MT, Helminen HJ, Jurvelin JS. Characterization of enzymatically induced degradation of articular cartilage using high frequency ultrasound. Phys Med Biol 1999;44:2723-2733.
40. Wang Q, Zheng YP, Qin L, Huang QH, Lam WL, Leung G, et al. Real-time ultrasonic assessment of progressive proteoglycan depletion in articular cartilage. Ultrasound Med Biol 2008;34:1085-1092.